



ISSN NO. 2320-5407

Journal homepage: <http://www.journalijar.com>

INTERNATIONAL JOURNAL
OF ADVANCED RESEARCH

RESEARCH ARTICLE

Study of optical properties of dicalcium- magnesium disilicate based phosphors doped rare earth material.

Ms. Dipti Pandey , Ravi Sharma , Nameeta Brahme
Civil Dep. / College of Engineering/University of Kufa/ Najaf/ IRAQ

Manuscript Info

Manuscript History:

Received: 12 October 2015
Final Accepted: 25 November 2015
Published Online: December 2015

Key words:

Thermo-luminescence (TL) , Photo-luminescence (PL)

*Corresponding Author

Ms. Dipti Pandey

Abstract

di-Calcium magnesium di-Silicate phosphor $\text{Ca}_2\text{MgSi}_2\text{O}_7$ doped different rare earth with white long-lasting afterglow was prepared by solid state reaction, and combustion method. Then after investigated its thermo luminescence & photoluminescence properties. The characteristic intra-configurational 4f emissions of rare earth were observed in the emission spectra as well as the afterglow spectra under ultraviolet excitation. The Thermoluminescence spectra above room temperature are employed for the discussion of the origin of traps .

Copy Right, IJAR, 2015,. All rights reserved

INTRODUCTION

Calcium magnesium silicate (CMS) has been studied as a host for long-lasting phosphor and plasma display panels (PDPs). The Eu^{2+} doped calcium magnesium silicate ($\text{CaMgSi}_2\text{O}_6$) or (CMS:Eu) is an efficient phosphor that emits blue light by the stimulation of ultraviolet or vacuum ultraviolet. Jiang et al. studied the luminescent properties of CMS-based phosphors co-doped with different rare-earth ions. Long lasting phosphorescence (LLP) can persist for a longtime in the darkness after the removal of the excitation. It has attracted much attention because it can be applied in many fields, such as emergency lighting, safety indication, road signs, luminous paints, graphic arts and other potential fields. Besides the blue, green and red long-lasting phosphors, the white long-lasting phosphors are also needed for full color display. Recently, the silicate long lasting phosphors have been focused because of their multi-color phosphorescence and resistance to acid, alkali and oxygen. Furthermore, the long-lasting phosphor $\text{Ca}_2\text{MgSi}_2\text{O}_7:\text{Eu}^{2+}$, Dy^{3+} has been investigated as a yellow phosphor, in which Dy^{3+} mainly act as trap centers. Thus, it has been suggested that $\text{Ca}_2\text{MgSi}_2\text{O}_7:\text{Dy}^{3+}$ may be novel white long- lasting phosphor.

It is essential to develop biocompatible, bioactive, bioresorbable and durable materials for orthopedic and dental implants, that are capable of bearing high stress and loads and that invoke positive cellular and genetic responses for the rapid repair, modification, regeneration and maintenance of the affected tissue in the human body. Silicate –based bioceramics, including silicate bioglass, akermanite $\text{Ca}_2\text{MgSi}_2\text{O}_7$ and $\text{Ca}_2\text{MgSi}_2\text{O}_8$ ceramics have been excellent apatite forming abilities in stimulated body fluids. Another remarkable observation of $\text{Ca}_2\text{MgSi}_2\text{O}_7:\text{Eu}^{2+}$ was a disagreement on the emission. The best persistent luminescent silicate is $\text{Sr}_2\text{MgSi}_2\text{O}_7:\text{Eu}^{2+}$, Dy^{3+} , but long afterglow has also been discovered in a number of silicate such as $\text{Ca}_2\text{MgSi}_2\text{O}_7:\text{Eu}^{2+}$ (Tb^{3+}) its fluorescence maximum(nm) is 515/535 (greenish) and afterglow maximum(nm) is idem.

2. Experimental:

A solid-state reaction at 1200–1400 °C is the most common way to prepare $\text{M}_2\text{MgSi}_2\text{O}_7$ samples, but recently combustion methods were also applied successfully.

Solid State Reaction Method

Samples with the general formula $(M_{1-x}Eu_x)_2MgSi_2O_7$ ($M = Ca$) were prepared by solid-state reactions. The starting reagents were $CaCO_3(AR)$, $MgO(AR)$, $SiO_2(AR)$, $Eu_2O_3(4N)$ and small quantities of H_3BO_3 were added as flux. The raw materials were weighted stoichiometrically and mixed thoroughly in an agate mortar, then sintered at $1100^\circ C$ for 3:30 h in a weak reductive atmosphere, followed by an additional grinding. Thus prepared is white powder.

Combustion Method

$CaCO_3, Mg(NO_3)_2, SiO_2 \cdot xH_2O, Eu(NO_3)_2, NH_4NO_3$ and Urea were mixed at a ratio of (1.96, 1, 2 0.04, 30, 35). All constituents in stoichiometric proportions, along with fuel and oxidizer were mixed together and small quantity of double distilled water was added. The mixture on thoroughly mixing was transferred to a pre-heated furnace at $600^\circ C$. On rapid heating the mixture evaporated and ignited at $450^\circ C$, with the evolution of a large amount of gases, to yield silicates. Entire process was completed within a few minutes. The as-prepared phosphors did not show intense emission, probably the activator Eu was not incorporated in divalent form. The phosphors were reheated, in the reducing atmosphere provided by heating in a closed box with char-coal, at $900^\circ C$ for 1h.

The crystalline structure of the sample was verified by x-ray powder diffraction (XRD), using a D/max-rA diffractometer (Cu-K α radiation at 1.5406 \AA) over the range $10-70^\circ$. The emission and excitation spectra were measured using a fluorescence spectrophotometer (RF-5301) with a Xe lamp as the excitation source. The afterglow decay curves were measured using the same equipments, but after irradiation with a mercury lamp ($\lambda_{ex} = 254 \text{ nm}$, low vapour pressure, $\sim 250 \mu W/cm^2$) for 5min. The thermo-luminescence (TL) glow curves of the samples were measured after irradiation with the same mercury lamp for 3 min at room temperature using a thermo-luminescence dosimeter (mode TLD I-001). All the measurements except for the thermo-luminescence curves were carried out at room temperature.

3. Result and Discussion:

3.1 Crystallization

The phase and structure morphology of the prepared samples were analyzed using XRD spectra SEM. For comparison, the XRD patterns shown in fig. 1 are those only for the samples with different doping materials (4 mol %) as well as different preparation techniques. It is observed from fig. 1 that the single-phased $Ca_2MgSi_2O_7 \cdot Dy^{3+}$ was obtained by solid state reaction under $1100^\circ C$. The structure of $Ca_2MgSi_2O_7 \cdot Dy^{3+}$ can be indexed to JCPDS number of 83-1815, corresponding to akermanite. The SEM images of prepared sample are shown in fig. b. From the SEM image it can be observed that the particle size distribution between 100nm and 500nm.

CALCULATION FOR CRYSTALLINE SIZE D_p & LATTICE INTERVAL d :

d calculated by Bragg's equation $n\lambda = d \sin\theta$ here $\lambda = 1.54 \text{ \AA}$

$Ca_2MgSi_2O_7 \cdot Dy$ 0.04

and Crystalline size D_p calculated by Scherrer's formula $D_p = K\lambda / \beta_{1/2} \cos\theta$

where K scherrer's constant = 0.94, $\beta_{1/2} \text{ FWHM} = 2\Delta\theta = 0.44^\circ = 0.00768 \text{ radian}$

Crystalline size $D_p = (0.94 \times 1.54056) / 0.00768 \times \cos(15.62)$
= 19.58 nm

$Ca_2MgSi_2O_7 \cdot Ce$ 0.04

d calculated by Bragg's equation $n\lambda = d \sin\theta$ here $\lambda = 1.54 \text{ \AA}$

and Crystalline size D_p calculated by Scherrer's formula $D_p = K\lambda / \beta_{1/2} \cos\theta$

where K scherrer's constant = 0.94, $\beta_{1/2} \text{ FWHM} = 2\Delta\theta = 0.44^\circ = 0.00768 \text{ radian}$

Crystalline size $D_p = (0.94 \times 1.54056) / 0.00768 \times \cos(16.7)$
= 19.69 nm

| $2\theta(\circ)$ | $\theta(\circ)$ | $\text{Sin}\theta(\text{degree})$ | I(a.u) | $d(\text{\AA}^\circ)$ |
|------------------|-----------------|-----------------------------------|--------|-----------------------|
| 23.28 | 11.64 | 0.2017617 | 166 | 7.63 |
| 24.02 | 12.01 | 0.208082 | 190 | 7.40 |
| 25.48 | 12.74 | 0.2205227 | 206 | 6.98 |
| 27.06 | 13.53 | 0.2339544 | 182 | 6.58 |
| 29.06 | 14.53 | 0.2508869 | 274 | 6.14 |
| 30.14 | 15.07 | 0.259998 | 308 | 5.92 |

| | | | | |
|-------|-------|------------|-------|------|
| 31.24 | 15.62 | 0.26925601 | 765 | 5.72 |
| 36.36 | 18.18 | 0.312003 | 167.8 | 4.94 |
| 45.54 | 22.77 | 0.3870328 | 170 | 3.98 |
| 51.92 | 25.96 | 0.437744 | 136 | 3.45 |

Ca₂MgSi₂O₇:Dy 0.04

Ca₂MgSi₂O₇:Ce 0.04

| 2θ(degree) | θ(degree) | Sinθ(degree) | I(a.u) | d (Å ^o) |
|------------|-----------|--------------|--------|---------------------|
| 21.88 | 10.94 | 0.1898 | 292.9 | 8.11 |
| 26.6 | 13.3 | 0.230 | 629.2 | 6.69 |
| 28.56 | 14.28 | 0.247 | 614 | 6.24 |
| 31.14 | 15.57 | 0.268 | 651.4 | 5.75 |
| 33.4 | 16.7 | 0.287 | 892 | 5.37 |
| 40.72 | 20.36 | 0.348 | 238 | 4.43 |
| 42.92 | 21.46 | 0.366 | 222.5 | 4.21 |
| 47.56 | 23.78 | 0.403 | 419.9 | 3.82 |
| 47.52 | 23.76 | 0.403 | 183.7 | 3.82 |
| 56.32 | 28.16 | 0.472 | 200.3 | 3.26 |

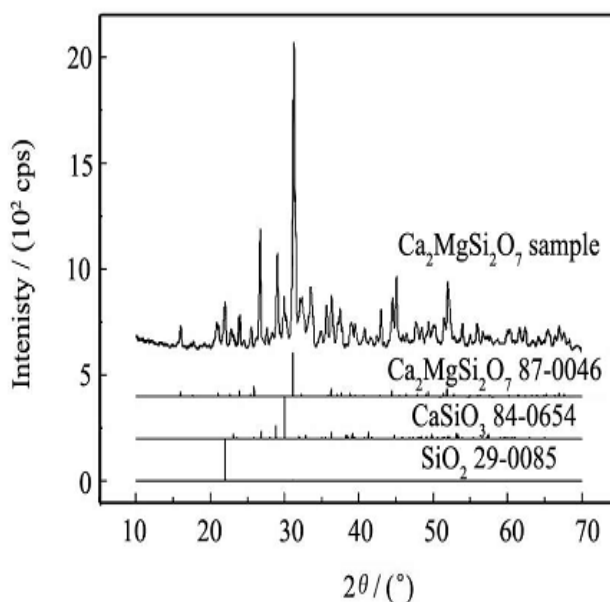


Fig.1 XRD pattern of Ca₂MgSi₂O₇: Dy³⁺ (4mol%)

4. Photo-luminescence Properties of the samples:

The excitation and emission spectra of different rare earth doped and undoped samples are shown in fig.2. The excitation spectrum of Ca₂MgSi₂O₇: Dy³⁺ consists of a strong broad band peaked at 240 nm, and several peaks ascribed to the 4f44f transitions of Dy³⁺, with the strongest one at 348 nm (⁶H_{15/2} → ⁶P_{7/2}). The Dy³⁺ emission (Fig.2 (a)) consists of three peaks at 479, 482, and 574 nm, which correspond to the transitions from ⁴F_{9/2} state to ⁶H_{15/2}, ⁶H_{13/2}, ⁶H_{11/2} and ⁶H_{9/2} states respectively. In addition, the strong excitation band at 260 nm is not presented in the similar Sr₂MgSi₂O₇: Dy³⁺. This strong excitation band can make the best use of energy of UV light from the sun, which is an advantage of this white long-lasting phosphor. The emission spectra are shown in figure 2. The emission spectra of Ca₂MgSi₂O₇: Eu²⁺ excited by 395 nm was observed & as seen from figure 3. The emission spectrum of Ca₂MgSi₂O₇: Eu²⁺ consists of three groups of emission peaking at 400, 577 and 602 nm. Emission in Sr₂MgSi₂O₇: Eu²⁺ (curve h) peaks at around 457 nm. Excitation spectrum of the Ca₂MgSi₂O₇: Eu²⁺ shows considerable intensity at 307 nm. The luminescence process of Eu²⁺-activated phosphor is characterized by the ⁴f₆ ⁵d → ⁴f₇ transition of Eu²⁺ acting as an activator centre. The absorption and emission due to the transition between ⁴f₇ and ⁴f₆ ⁵d states of Eu²⁺ strongly depend on host material, cations replaceable by Eu²⁺ in the host matrix and the

crystal field acting on Eu^{2+} . The photoluminescence spectra of the two samples are shown in Fig. The main emission peaks are at 470 and 535 nm, respectively. The emission is typical for that of Eu^{2+} ascribed to $4f - 5d$ transitions. Under these excitation wave lengths, however, no emission of Eu^{3+} and Dy^{3+} was observed. However, we have recently observed for the first time emission of Dy^{3+} using synchrotron VUV radiation excitation. This means that Dy^{3+} in these Eu – Dy co-doped systems acts not only as a trap but also as a luminescence centre.

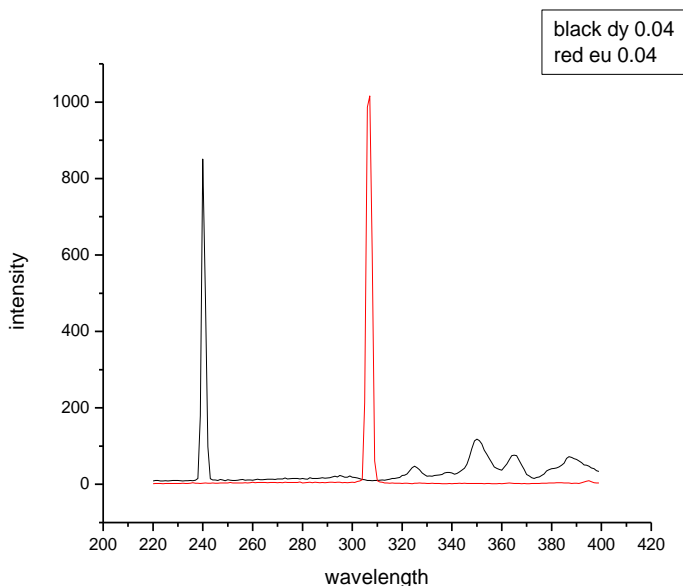


Fig2(a) Excitation Spectra of $\text{Ca}_2\text{MgSi}_2\text{O}_7:\text{Dy}^{3+}$ ($\lambda_{\text{em}}=481\text{nm}$) and fig (b) Excitation Spectra $\text{Ca}_2\text{MgSi}_2\text{O}_7:\text{Eu}^{2+}$ ($\lambda_{\text{em}}=615\text{nm}$).

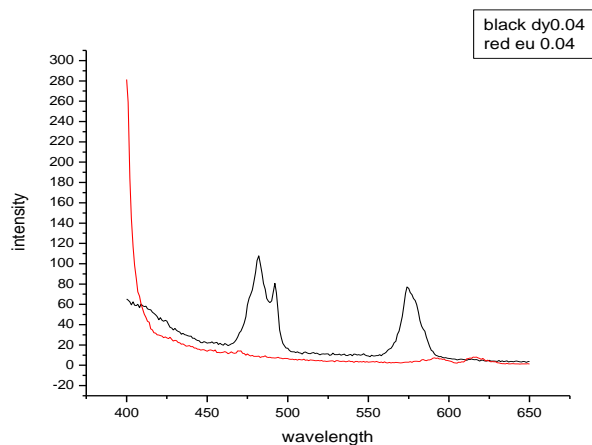


Figure 3. Emission spectra for Eu^{2+} doped disilicate a $\text{Ca}_2\text{MgSi}_2\text{O}_7$ excited by 348nm, b. $\text{Ca}_2\text{MgSi}_2\text{O}_7:\text{Dy}^{3+}$ excited by 395 nm .

5. Thermo-luminescence properties of the samples:

Usually information of trapping level and thermal depth of trap can be obtained by thermo-luminescence curve. Fig (a) is the TL curve of the Eu^{2+} doped disilicate a $\text{Ca}_2\text{MgSi}_2\text{O}_7$ and fig (b) is the TL curve of the $\text{Ca}_2\text{MgSi}_2\text{O}_7:\text{Dy}^{3+}$. The TL curve of $\text{Ca}_2\text{MgSi}_2\text{O}_7:\text{Eu}^{2+}$, $\text{Ca}_2\text{MgSi}_2\text{O}_7:\text{Dy}^{3+}$ were studied after irradiation with mercury lamp at room temperature are recorded and From the fig (a) it can be observed that a broad TL band from in the range from 323K

to 500K. One TL peak at 371K can be found. While fig (b) shows that TL band from in the range of temperature 323K to 600K. By **thermal cleaning technique**, two bands peaked at 367.62K and 565.18K were both separated from the TL curve.

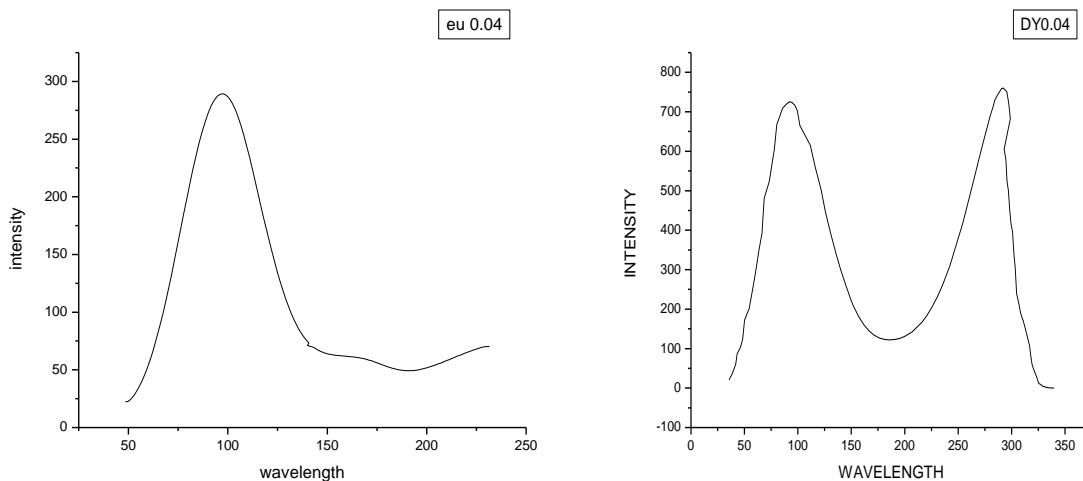


Figure 6.(a)Thermo- luminescence spectra of $\text{Ca}_2\text{MgSi}_2\text{O}_7:\text{Eu}^{2+}$ (b)Thermo- luminescence spectra of $\text{Ca}_2\text{MgSi}_2\text{O}_7:\text{Dy}^{3+}$

Conclusion:

Both $\text{Ca}_2\text{MgSi}_2\text{O}_7:\text{Eu}^{2+}$ and $\text{Ca}_2\text{MgSi}_2\text{O}_7:\text{Dy}^{3+}$ have akermanite structures. The photoluminescence study of these materials show the strong emission of Eu^{2+} in alkaline earth silicates which agrees well with the literature. The bio- compatibility of the akermanite has already been reported by many researchers. The luminescence properties of these bio- materials may be useful in their use as biomarkers and in the controlled drug delivery. a series of silicate compounds, $\text{Ca}_x\text{MgSi}_2\text{O}_{5+x}:\text{Dy}^{3+}$ ($x = 1, 2, 3$), with white long afterglow after irradiation with the mercury lamp have been prepared. The white afterglow comes from the combination of the yellow and the blue emissions corresponding to the transitions between 4f levels of the doping Dy^{3+} ions. The white afterglow can last for one hour for most of the samples prepared, suggesting promising candidates for the development of the white long afterglow phosphors.

References:

- [1] T. Matsuzawa, Y. Aoki, N. Takeuchi, Y. Murayama, J. Electrochem. Soc. 143 (1996) 2670.
- [2] S. Uehara, Y. Ochi, US Patent 6,284,156, 2001.
- [3] P. Dorenbos, J. Electrochem. Soc. 152 (2005) H107.
- [4] B. Lei, Y. Liu, Z. Ye, C. Shi, Chin. Chem. Lett. 15 (2004) 335.
- [5] Y. Liu, B. Lei, C. Shi, Chem. Mater. 17 (2005) 2108.
- [6] J. Kuang, Y. Liu, J. Zhang, J. Solid State Chem. 179 (2006) 266.
- [7] B. Liu, C. Shi, Z. Qi, Appl. Phys. Lett. 86 (2005) 19 1111.
- [8] B. Liu, L. Kong, C. Shi, J. Lumin. 122–123 (2007) 121.
- [9] B. Liu, C. Shi, Z. Qi, J. Phys. Chem. Solids. 67 (2006) 1674.
- [10] L. Jiang, C. Chang, D. Mao, J. Alloys Compd. 260 (2003) 193.
- [11] Y. Lin, Z. Zhang, Z. Tang, X. Wang, J. Zhang, Z. Zheng, J. Eur. Ceram. Soc. 21 (2001) 683.
- [12] Bhatkar V B, Omanwar S K and Moharil S V 2002 Phys. Status Solidi (a) 191 272

- [13]Bhatkar V B, Omanwar S K and Moharil S V 2007 Opt. Mater. 29,1066
- [14]Blasse G et al 1968 Philips Res. Rep. 23 189
- [15]Cerruti M and Sahai N 2006Rev. Mineral. Geochem. 64 283
- [16]Chandrappa G T, Ghosh S and Patil K C 1999 J. Mater. Synth. Process. 7 273
- [17]Dora A, Hernández C, Luis A, Aragón B, Lara W O, Rentería- Zamarrón D and Salinas-Delgado Y 2008 Bioceramics 21 527.
- [18]Ekambaram S and Patil K C 1995 Bull. Mater. Sci. 18 921
- [19]Kuang J. Y,Liu Y.L.White emitting long-lasting phosphor $\text{Sr}_2\text{SiO}_4:\text{Dy}^{3+}$.Chem. Lett.,2005,34(4):598
- [20]Liu Y.L,Lei B.F,Shi C.S.Luminescent properties of a white Afterglow phosphor $\text{CdSiO}_3:\text{Dy}^{3+}$.Chem.Mater.,2005,17(8): 2108.